



Electrical transport and magnetoresistance in $\text{La}_{2/3}\text{Ca}_{1/3}\text{MnO}_3/\text{BaZrO}_3$ composites

Ling Gao^a, Lifeng Bai^a, Chengshan Li^a, Xianghong Liu^a, Zhanwen Wu^b, Dongning Zheng^b, Yafeng Lu^{a,*}

^a Northwest Institute for Nonferrous Metal Research, P.O. Box 51, Xi'an, Shaanxi 710016, PR China

^b Beijing National Laboratory for Condensed Matter Physics, Institute of Physics, Chinese Academy of Sciences, Beijing 100080, PR China

ARTICLE INFO

Article history:

Received 17 September 2008

Received in revised form

27 December 2011

Accepted 4 January 2012

Available online 13 January 2012

Keywords:

Composite

Percolation conduction

$\text{La}_{2/3}\text{Ca}_{1/3}\text{MnO}_3$

BaZrO_3

ABSTRACT

We report the results of electrical resistivity and magnetoresistance (MR) measurements carried out on $\text{La}_{2/3}\text{Ca}_{1/3}\text{MnO}_3/\text{BaZrO}_3$ composites prepared by solid state reaction method. The metal-to-insulator transition and the magnitude of magnetoresistance are significantly influenced by the content of BaZrO_3 , suggesting the presence of ionic diffusion between $\text{La}_{2/3}\text{Ca}_{1/3}\text{MnO}_3$ and BaZrO_3 , although the dependence of the electrical resistivity as a function of $\text{La}_{2/3}\text{Ca}_{1/3}\text{MnO}_3$ volume fraction can be roughly described by classical percolation conduction model. The conductive behavior above the metal-to-insulator transition temperature can be well explained by Mott's variable range hopping model.

© 2012 Elsevier B.V. All rights reserved.

1. Introduction

Much attention has been paid on perovskite oxides during the last decades because they have rich physical properties including superconductivity with high- T_C , ferromagnetism with half metallicity, and ferroelectricity with large polarizations, etc. For manganite-based perovskite oxides of $\text{La}_{1-x}\text{A}_x\text{MnO}_3$ with an optimal doping content the colossal magnetoresistance (CMR) is observed when a high magnetic field is applied. The magnetoresistance effect is greatly influenced by the presence of grain boundaries in polycrystalline materials [1,2] and the lattice mismatch strain in heteroepitaxial films [3,4]. For potential applications in spintronics devices a large magnetoresistance effect at low applied magnetic field is necessary. A lot of efforts have been devoted to achieve low-field magnetoresistance in magnetic tunnel junctions (MTJs) with insulating barrier [5–12], in artificial bicrystal grain boundary junctions [13–18] and in manganite/insulating oxide composites [19–24]. In magnetic tunnel junctions the tunneling magnetoresistance (TMR) effect is principally dependent on the spin polarization of ferromagnetic electrodes and the spin-dependent tunneling process through insulating barrier. For the artificial bicrystal grain boundary junctions, isolated grain boundary effect on low field magnetoresistance can be investigated. Well-defined manganite/barrier interface and manganite grain boundary structure must be obtained in both cases above.

Usually conventional solid state reaction is employed to prepare manganite/insulating oxide composites, where the secondary insulating phase is assumed to be chemically immiscible with the manganite matrix. Enhanced spin-dependent scattering of conductive electrons at manganite/oxide phase boundary is expected to contribute to low-field magnetoresistance effect in the composites. In $\text{La}_{2/3}\text{Sr}_{1/3}\text{MnO}_3/\text{CeO}_2$ composite the magnetoresistance of 1.5% at 100 Oe was observed for the sample with a percolation threshold of $\text{La}_{2/3}\text{Sr}_{1/3}\text{MnO}_3$ volume fraction ($f_{\text{LSMO}} = 0.20$) [25], which is close to the critical volume fraction theoretically predicted for usual three-dimensional lattice types [26]. Similar experimental results for the manganite/insulating oxide composites were reported [21]. In the real systems, possible ionic diffusion between the phases, however, is important for both theoretical and experimental aspects for understanding behavior of conductivity for composite materials. We present detailed preparation, electrical transport and magnetoresistance studies of the $\text{La}_{2/3}\text{Ca}_{1/3}\text{MnO}_3/\text{BaZrO}_3$ composite. We observe that the effect of ionic interdiffusion between the $\text{La}_{2/3}\text{Ca}_{1/3}\text{MnO}_3$ (LCMO) and BaZrO_3 secondary phase (BZO) should be taken into account for explanation of transport properties.

2. Experiment

Conventional solid state reaction in air was used to prepare $\text{La}_{2/3}\text{Ca}_{1/3}\text{MnO}_3$ bulks. These starting powders of La_2O_3 , CaCO_3 and MnO_2 (99.5% purity) were mixed and heated at 1000 °C for 36 h in air with intermediate grinding. Cold-pressed pellets were then sintered at 1400 °C for 12 h with furnace cooling. For preparation of polycrystalline (x)LCMO:(1-x)BZO samples with different $\text{La}_{2/3}\text{Ca}_{1/3}\text{MnO}_3$ volume fractions x, milled LCMO powder was thoroughly mixed and grounded with BaZrO_3 powder. The mixture was finally sintered at 1300–1400 °C for 24 h in air.

* Corresponding author. Tel.: +86 29 86231079; fax: +86 29 86224487.

E-mail address: yflu@c-nin.com (Y. Lu).

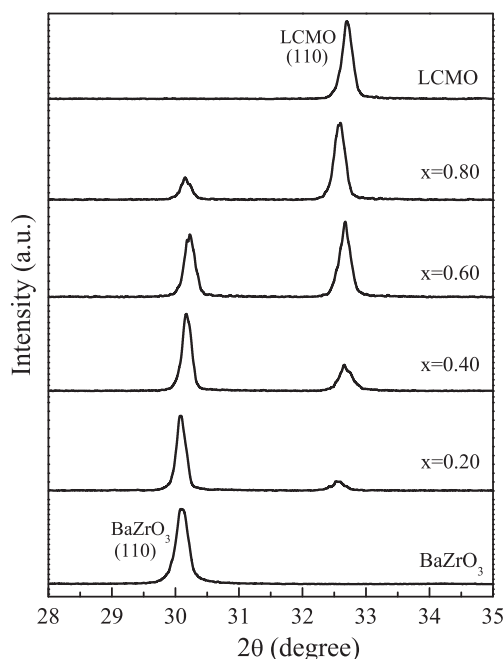


Fig. 1. XRD pattern for $(x)\text{La}_{2/3}\text{Ca}_{1/3}\text{MnO}_3:(1-x)\text{BaZrO}_3$ composites with different $\text{La}_{2/3}\text{Ca}_{1/3}\text{MnO}_3$ volume fraction x .

The phase composition and the crystalline quality of the $\text{La}_{2/3}\text{Ca}_{1/3}\text{MnO}_3$ and composites were analyzed employing X-ray diffraction (XRD) using $\text{Cu-K}\alpha$ radiation. The micrograph of samples was investigated by scanning electric microscopy (SEM). Resistivity dependent on temperature from 77 K to 300 K was measured by standard four-probe method in zero field and 0.6 T applied magnetic field to evaluate electrical and magnetoresistance properties for bar-shaped samples. The magnetoresistance (MR) is defined as $\text{MR} = (R(0) - R(H))/R(0)$, where $R(0)$ is the resistivity in zero magnetic field and $R(H)$ is the resistivity in applied magnetic field of 0.6 T.

3. Results and discussion

X-ray powder diffraction result on $\text{La}_{2/3}\text{Ca}_{1/3}\text{MnO}_3$ in Fig. 1 demonstrates a pure perovskite phase within the experimental error. For $(x)\text{La}_{2/3}\text{Ca}_{1/3}\text{MnO}_3:(1-x)\text{BaZrO}_3$ composites, no impurity phase peaks except for diffraction peaks of the $\text{La}_{2/3}\text{Ca}_{1/3}\text{MnO}_3$ and BaZrO_3 phase were detected. The relative intensities of diffraction peaks from the LCMO phase systematically change with the LCMO volume fraction. We notice that the (110) diffraction peak positions of the $\text{La}_{2/3}\text{Ca}_{1/3}\text{MnO}_3$ phase have a rather slight shift towards low-angle direction with increasing the BaZrO_3 content, whereas the (110) diffraction peak of the BaZrO_3 phase moves towards high-angle direction. This suggests the presence of interdiffusion between Mn^{3+} and Zr^{4+} discussed later. It is actually difficult to get a complete chemical immiscibility between $\text{La}_{2/3}\text{Ca}_{1/3}\text{MnO}_3$ and BaZrO_3 if usual solid state reaction method is employed, although the ionic diffusion between the $\text{La}_{2/3}\text{Ca}_{1/3}\text{MnO}_3$ and BaZrO_3 phases does not lead to formation of impurity phases in the composites.

Fig. 2 gives SEM images of the $(x)\text{La}_{2/3}\text{Ca}_{1/3}\text{MnO}_3:(1-x)\text{BaZrO}_3$ composites to study morphology evolution with introduction of BaZrO_3 . Pure $\text{La}_{2/3}\text{Ca}_{1/3}\text{MnO}_3$ has a typical equiaxed microstructure with an average grain size of $\sim 4\ \mu\text{m}$. Upon addition of 10% BaZrO_3 the microstructure of the composite is apparently changed, where a lot of small grains are detectable. Further increasing the BaZrO_3 volume fraction obviously leads to formation of microstructure with homogenous fine grains with an average size of 0.4–0.5 μm . For the $x = 0.2$ sample, however, sudden coarsening is controlled by the growth behavior of BaZrO_3 itself. We believe that in the $(x)\text{La}_{2/3}\text{Ca}_{1/3}\text{MnO}_3:(1-x)\text{BaZrO}_3$ system the introduction of BaZrO_3 significantly suppresses the growth of $\text{La}_{2/3}\text{Ca}_{1/3}\text{MnO}_3$

grains due to blocking of movement of the grain boundaries. This kind of refined grain microstructure will affect the electrical transport property in these composites.

We measured temperature dependent resistivity curves in zero and 0.6 T applied magnetic field for a series of specimens with varying x . For $x > 0.23$ we observe an obvious metal-to-insulator transition. In Fig. 3 representative resistivity curves dependent on temperature for $(x)\text{La}_{2/3}\text{Ca}_{1/3}\text{MnO}_3:(1-x)\text{BaZrO}_3$ composites are plotted. The transition peak temperature is denoted as T_p . On the contrary, the samples with $x < 0.23$ do not display any resistive transition in the measured temperature and resistance range.

Fig. 4 indicates the transition peak temperature T_p with different LCMO volume fractions for the composites. With addition of a little amount of BaZrO_3 the T_p of the composite significantly drops down to 125 K for $x = 0.90$. Further increasing the BZO content gives rise to a slightly rising of T_p , but the T_p value is only around 180 K for $x \sim 0.40$. The T_p drop in the LCMO/BZO composite is much larger than that in other manganite/insulator composites [27,21]. This can be attributed to a possible variation of the manganite composition due to the existence of ionic interdiffusion between the phases. The reversible increase in T_p with decreasing the LCMO content for $x < 0.90$ implies that the ionic interdiffusion occurs mainly at the interface of the $\text{La}_{2/3}\text{Ca}_{1/3}\text{MnO}_3$ and BaZrO_3 phases. The magnetoresistance of the composite shows a reverse trend with the volume fraction of BaZrO_3 , i.e. the MR increases with decreasing the T_p similar to the effects induced by element substitution [28] and lattice strain [4].

Fig. 5 shows the resistivity of the composites at 300 K as a function of the $\text{La}_{2/3}\text{Ca}_{1/3}\text{MnO}_3$ volume fraction. A sharp increase of five orders of magnitude in the resistivity of composites was detected at $x \sim 0.20$ in the measured range. The classical percolation law is usually used to evaluate the conductive process for the conductive regime. According the percolation law $\rho \propto (f - f_c)^{-t}$, [29] the percolation threshold f_c the resistivity exponent t fitted to the measured data are 0.195 and 1.9, which actually fall in the range of theoretical predications of three-dimensional continuum percolation models. The 0.195 percolation threshold basically agrees with the value found for $\text{La}_{2/3}\text{Sr}_{1/3}\text{MnO}_3/\text{CeO}_2$ composites ($f_{\text{LSMO}} = 0.20$) [21]. Because many factors, such as porosity, poor connectivity, grain size difference and composition variation, affect the percolation conductive behavior in conducting/insulating composites, we should point out that the fitting does not fully confirm the presence of pure percolative conductivity in the $\text{La}_{2/3}\text{Ca}_{1/3}\text{MnO}_3/\text{BaZrO}_3$ composites, where the apparent decrease of the transition peak temperature T_p with the introduction of BaZrO_3 is an indicator of composition variation in the $\text{La}_{2/3}\text{Ca}_{1/3}\text{MnO}_3$.

It has been found above that the electronic conduction at high T with the $\text{La}_{2/3}\text{Ca}_{1/3}\text{MnO}_3$ volume fraction follows the classical 3D continuum model for the LCMO/BZO composite. In order to explore the conductive mechanism above T_p we analyze the temperature dependent resistivity for the composites. For the pure $\text{La}_{2/3}\text{Ca}_{1/3}\text{MnO}_3$ sintered bulk the electronic conduction above T_p can be usually described by the thermal activation model $\rho = \rho_\infty \exp(E_0/kT)$ [21]. For the LCMO/BZO composite it was not successful to fit the $\rho(T)$ data above T_p by the thermal activation model. The measured data in the relatively wide temperature range are well fitted by the variable range hopping (VRH) model $\rho = \rho_0 \exp[(T_0/T)^{1/4}]$ proposed by Mott [30]. Fig. 6 displays several typical results for $f_{\text{LCMO}} = 0.23, 0.30, 0.70$ and 0.90 . We find that the slope obtained from the relationship between $\ln \rho$ and $T^{-1/4}$ as shown in Fig. 6 is almost identical for different x , suggesting that increasing the BZO content does not lead to a change of electronic conduction mechanism in the composite. This also indicated a very low and limited solution of BaZrO_3 in $\text{La}_{2/3}\text{Ca}_{1/3}\text{MnO}_3$. Based on consideration of the tendency of the T_p and MR as indicated in Fig. 4, we believe that the ionic diffusion, especially at the phase interface,

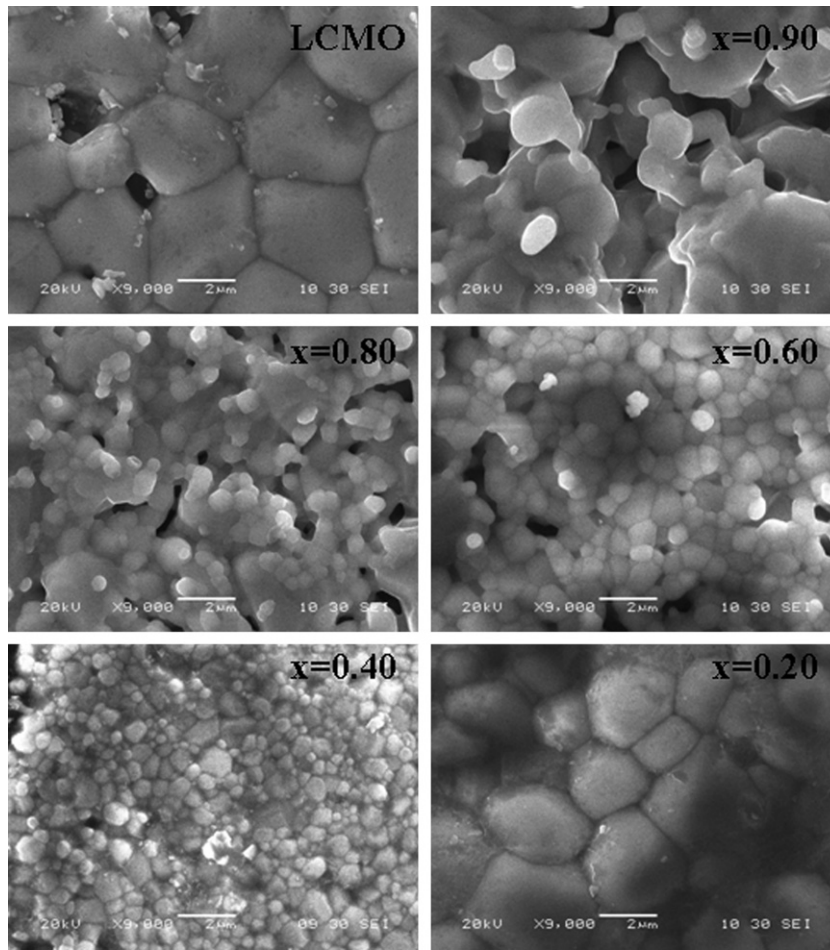


Fig. 2. SEM images of $(x)\text{La}_{2/3}\text{Ca}_{1/3}\text{MnO}_3:(1-x)\text{BaZrO}_3$ sintered bulks.

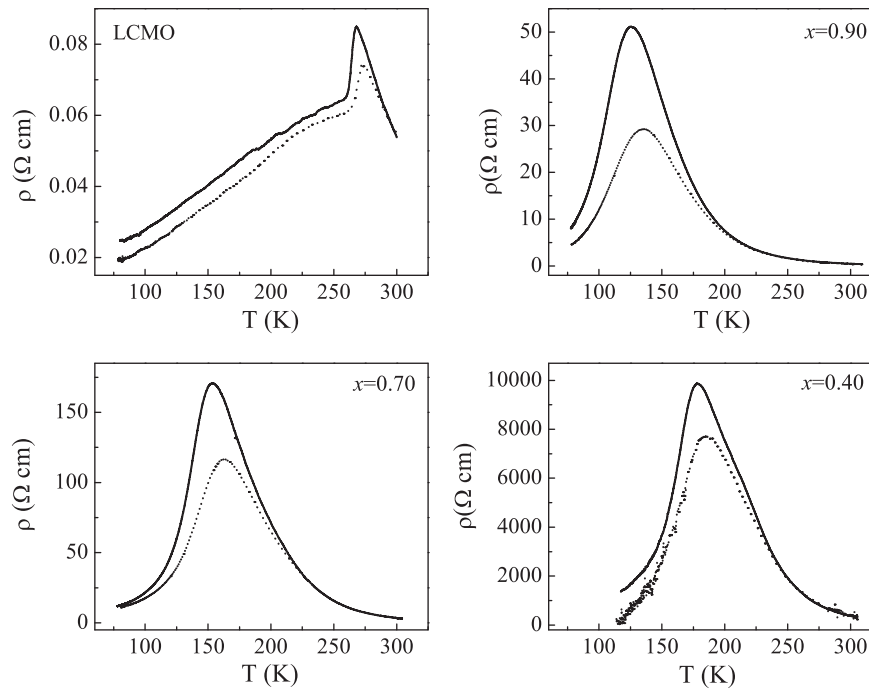


Fig. 3. Temperature-dependent resistivity curves for $(x)\text{La}_{2/3}\text{Ca}_{1/3}\text{MnO}_3:(1-x)\text{BaZrO}_3$ composites measured at zero field (solid lines) and 0.6 T (dotted lines).

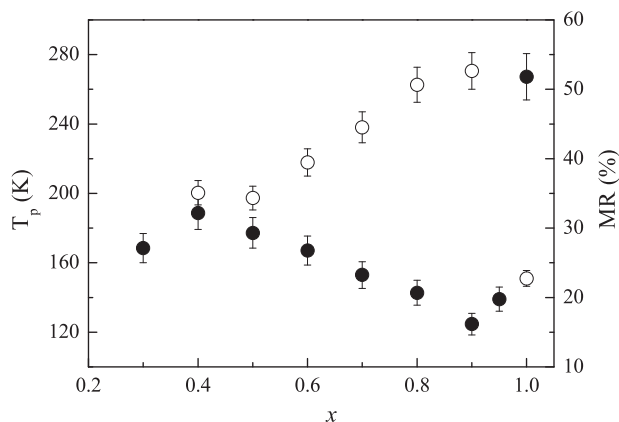


Fig. 4. Metal-to-insulator transition temperature T_p (solid circles) and magnetoresistance MR (open circles) dependent on the $\text{La}_{2/3}\text{Ca}_{1/3}\text{MnO}_3$ volume fraction x . The MR was measured at 0.6 T and given at near T_p , i.e. the maximal MR value.

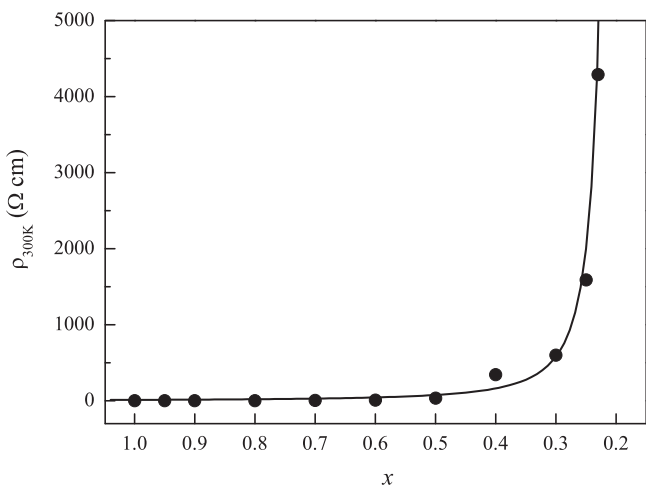


Fig. 5. Electrical resistivity at 300 K as a function of the $\text{La}_{2/3}\text{Ca}_{1/3}\text{MnO}_3$ volume fraction x . The line corresponds to the fit by percolation law.

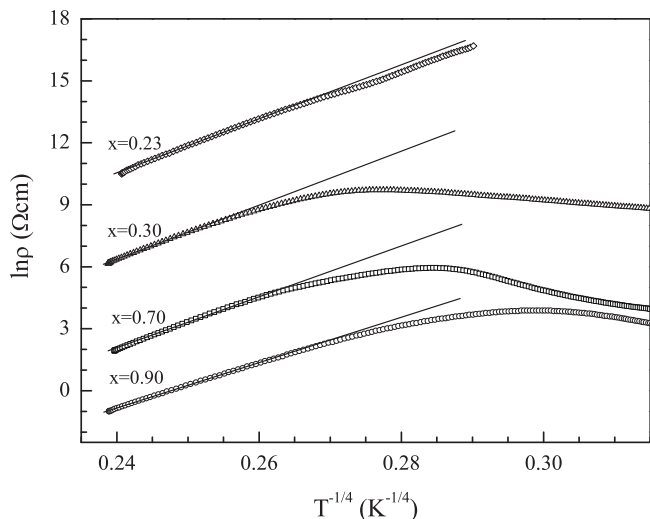


Fig. 6. $\ln \rho$ is plotted versus $T^{-1/4}$ for some representative $(x)\text{La}_{2/3}\text{Ca}_{1/3}\text{MnO}_3-(1-x)\text{BaZrO}_3$ composites. The lines are linear fits to the data by the formula $\rho = \rho_0 \exp[(T_0/T)^{1/4}]$ above T_p .

is responsible for the VRH-type conductivity in the LCMO/BZO composite. The ionic diffusion limited at the LCMO/BZO phase interface may give rise to random potential fluctuations, which localize the carriers in the LCMO.

Substitutive ionic diffusion in the LCMO/BZO composite occurs most probably between Mn^{3+} and Zr^{4+} . The probability of the $\text{Mn}^{3+}/\text{Zr}^{4+}$ interdiffusion should have a maximum at the phase interface. For the high f_{LCMO} composite the BaZrO_3 easily distributes homogeneously at the grain boundaries of $\text{La}_{2/3}\text{Ca}_{1/3}\text{MnO}_3$, resulting in a heavy diffusion. The Mn^{3+} composition variation due to the ionic diffusion will be unfavorable to the double-exchange interaction, and the metal-to-insulator transition is thus suppressed. In the meantime, this kind of ionic interdiffusion can lead to a change of high-temperature conductivity mechanism like that of Mn-site doping effects. Although the limited ion substitution greatly has changed the metal-to-insulator transition temperature and corresponding high-temperature conductivity in the composites, the refined grain microstructure by addition of BaZrO_3 makes the system to keep three-dimensional continuum percolation behavior. It should be pointed out that a large low-field magnetoresistance of 53% in 0.6 T for the $x = 0.90$ composite was found, which is beneficial to practical applications for CMR materials.

4. Conclusion

We have prepared the $\text{La}_{2/3}\text{Ca}_{1/3}\text{MnO}_3/\text{BaZrO}_3$ composites by conventional solid state reaction method. The electrical and magnetoresistance properties of the composites have been investigated. Remarkable changes of metal-to-insulator transition temperature, low-field magnetoresistance and high-temperature resistivity behavior were observed, suggesting importance of the variation of the manganite composition due to ionic interdiffusion in the $\text{La}_{2/3}\text{Ca}_{1/3}\text{MnO}_3/\text{BaZrO}_3$ composites. However, the refined grain microstructure by due to suppression of the $\text{La}_{2/3}\text{Ca}_{1/3}\text{MnO}_3$ growth by addition of BaZrO_3 makes the system to keep 3D continuum percolation behavior at room temperature.

Acknowledgment

This work was financially supported by the National Science Fund Program of China (grant no. 50872115).

References

- [1] H.Y. Hwang, S-W. Cheong, N.P. Ong, B. Batlogg, Phys. Rev. Lett. 77 (1996) 2041–2044.
- [2] C. Srinithiwarawang, M. Ziese, Appl. Phys. Lett. 73 (1998) 1140–1143.
- [3] S. Jin, T.H. Tiefel, M. McCormack, R.A. Fastnacht, R. Ramesh, L.H. Chen, Science 264 (1994) 413–415.
- [4] Y. Lu, J. Klein, F. Herbristrit, J.B. Philipp, A. Marx, R. Gross, Phys. Rev. B 73 (2006) 184406.
- [5] Y. Lu, X.W. Li, G.Q. Gong, G. Xiao, A. Gupta, P. Lecoeur, J.Z. Sun, Y.Y. Wang, V.P. Dravid, Phys. Rev. B 54 (1996) R8357–R8360.
- [6] J.Z. Sun, W.J. Gallagher, P.R. Duncombe, L. Krusin-Elbaum, R.A. Altman, A. Gupta, Y. Lu, G.Q. Gong, G. Xiao, Appl. Phys. Lett. 69 (1996) 3266–3269.
- [7] M. Viret, M. Drouet, J. Nassar, J.P. Contour, C. Fermon, A. Fert, Europhys. Lett. 39 (1997) 545–551.
- [8] M.-H. Jo, N.D. Mathur, N.K. Todd, M.G. Blamire, Phys. Rev. B 61 (2000) R14905–R14908.
- [9] A. Gupta, J.Z. Sun, J. Magn. Magn. Mater. 200 (1999) 24–43.
- [10] J.Z. Sun, Physica C 350 (2001) 215–226.
- [11] P.K. Wong, J.E. Evetts, M.G. Blamire, Phys. Rev. B 62 (2000) 5821–5828.
- [12] Y. Lu, J. Appl. Phys. 102 (2007) 123906.
- [13] N.D. Mathur, G. Burnell, S.P. Isaac, T.J. Jackson, B.-S. Teo, J.L. MacManus-Driscoll, L.F. Cohen, J.E. Evetts, M.G. Blamire, Nature 387 (1997) 266–268.
- [14] K. Steenbeck, T. Eick, K. Kirsch, K. O'Donnell, E. Steinbeiß, Appl. Phys. Lett. 71 (1997) 968–971.
- [15] J. Klein, C. Höfener, S. Uhlenbruck, L. Alff, B. Büchner, R. Gross, Europhys. Lett. 47 (1999) 371–378.
- [16] R. Gross, L. Alff, B. Büchner, B.H. Freitag, C. Höfener, J. Klein, W. Yafeng Lu, J.B. Mader, M.S.R. Philipp, P. Rao, S. Reutler, S. Ritter, S. Thienhaus, B. Uhlenbruck, Wiedenhorst, J. Magn. Magn. Mater. 211 (2000) 150–159.

- [17] C. Höfener, J.B. Philipp, J. Klein, L. Alff, A. Marx, R. Gross, *Europhys. Lett.* 50 (2000) 681–688.
- [18] J.B. Philipp, C. Höfener, S. Thienhaus, J. Klein, L. Alff, R. Gross, *Phys. Rev. B* 62 (2000) R9248–R9251.
- [19] D. Das, A. Saha, C.M. Srivastava, R. Raj, S.E. Russek, D. Bahadur, *J. Appl. Phys.* 95 (2004) 7107–7108.
- [20] P. Kameli, H. Salamati, M. Eshraghi, M.R. Mohammadizadeh, *J. Appl. Phys.* 98 (2005) 043908.
- [21] B. Vertruyen, R. Cloots, M. Ausloos, J.-F. Fagnard, Ph. Vanderbemden, *Phys. Rev. B* 75 (2007) 165112.
- [22] Z.Y. Zhou, X.S. Wu, J. Du, S. Xu, X.J. Bai, G.S. Luo, F.Y. Jiang, *Acta. Metal. Sinica* 22 (2009) 51–57.
- [23] B.X. Huang, Y.H. Liu, X.B. Yuan, C.J. Wang, R.Z. Zhang, L.M. Mei, *J. Magn. Magn. Mater.* 280 (2004) 176–183.
- [24] J.H. Miao, S.L. Yuan, G.M. Ren, X. Xiao, G.Q. Yu, *J. Rare. Earth* 25 (2007) 204–209.
- [25] L. Balcells, A.E. Carrillo, B. Martinez, J. Fontcuberta, *Appl. Phys. Lett.* 74 (1999) 4014–4017.
- [26] H. Scher, R. Zallen, *J. Chem. Phys.* 53 (1970) 3759–3761.
- [27] S. Park, N. Hur, S. Guha, S.-W. Cheong, *Phys. Rev. Lett.* 92 (2004) 167206.
- [28] K. Khazeni, Y.X. Jiam, L. Lu, V.H. Crespi, M.L. Cohen, A. Zettl, *Phys. Rev. Lett.* 76 (1996) 295–298.
- [29] B.I. Shklovskii, A.L. Efros, *Electronic Properties of Doped Semiconductors*, Springer, New York, 1984.
- [30] N.F. Mott, *Philos. Mag.* 19 (1969) 835–852.